NTIS HC #4.25

AD-754 771

Magnetospheric Electron Density Measurements from Upper Hybrid Resonance Noise Observed by IMP-6

by

Robert R. Shaw
and
Donald A. Gurnett

Department of Physics and Astronomy

THE UNIVERSITY OF IOWA

Iowa City, Iowa

U. of Iowa/72-37

Magnetospheric Electron Density Measurements from Upper Hybrid Resonance Noise Observed by IMP-6

by

Robert R. Shaw
and
Donald A. Gurnett

Department of Physics and Astronomy
The University of Iowa
Iowa City, Iowa 52240

December 1972

This work was supported in part by the National Aeronautics and Space Administration under Contracts NAS5-11074 and Grant NGL-16-001-043 and by the Office of Naval Research under Grant N00014-68-A-0196-0003.

UNCLASSIFIED

Security Classification

DOCUMENT CONTROL DATA - R&D

(Security classification of title, body of abstract and indexing annotation must be entered when the overall report is classified)

1. ORIGINATING ACTIVITY *(Corporate author)*

Department of Physics and Astronomy
University of Iowa

2a. REPORT SECURITY CLASSIFICATION

UNCLASSIFIED

2b. GROUP

3. REPORT TITLE

"Magnetospheric Electron Density Measurements from Upper Hybrid Resonance Noise Observed by IMP-6"

4. DESCRIPTIVE NOTES *(Type of report and inclusive dates)*

Progress, December 1972

5. AUTHOR(S) *(Last name, first name, initial)*

Shaw, Robert R, and D. A. Gurnett

6. REPORT DATE	7a. TOTAL NO. OF PAGES	7b. NO. OF REFS
December 1972	43	24

8a. CONTRACT OR GRANT NO.	9a. ORIGINATOR'S REPORT NUMBER(S)
N00014-68-A-0196-0003	U. of Iowa 72-37
b. PROJECT NO.	
c.	9b. OTHER REPORT NO(S) *(Any other numbers that may be assigned this report)*
d.	

10. AVAILABILITY/LIMITATION NOTICES

Approved for public release; distribution is unlimited.

11. SUPPLEMENTARY NOTES	12. SPONSORING MILITARY ACTIVITY
	Office of Naval Research

13. ABSTRACT

[See following page]

DD FORM 1 JAN 64 1473

UNCLASSIFIED

Security Classification

14. KEY WORDS	LINK A		LINK B		LINK C	
	ROLE	WT	ROLE	WT	ROLE	WT
Upper Hybrid Resonance Noise						
Magnetospheric Electron Density						
Cerenkov Radiation						

INSTRUCTIONS

1. ORIGINATING ACTIVITY: Enter the name and address of the contractor, subcontractor, grantee, Department of Defense activity or other organization *(corporate author)* issuing the report.

2a. REPORT SECURITY CLASSIFICATION: Enter the overall security classification of the report. Indicate whether "Restricted Data" is included. Marking is to be in accordance with appropriate security regulations.

2b. GROUP: Automatic downgrading is specified in DoD Directive 5200.10 and Armed Forces Industrial Manual. Enter the group number. Also, when applicable, show that optional markings have been used for Group 3 and Group 4 as authorized.

3. REPORT TITLE: Enter the complete report title in all capital letters. Titles in all cases should be unclassified. If a meaningful title cannot be selected without classification, show title classification in all capitals in parenthesis immediately following the title.

4. DESCRIPTIVE NOTES: If appropriate, enter the type of report, e.g., interim, progress, summary, annual, or final. Give the inclusive dates when a specific reporting period is covered.

5. AUTHOR(S): Enter the name(s) of author(s) as shown on or in the report. Enter last name, first name, middle initial. If military, show rank and branch of service. The name of the principal author is an absolute minimum requirement.

6. REPORT DATE: Enter the date of the report as day, month, year; or month, year. If more than one date appears on the report, use date of publication.

7a. TOTAL NUMBER OF PAGES: The total page count should follow normal pagination procedures, i.e., enter the number of pages containing information.

7b. NUMBER OF REFERENCES: Enter the total number of references cited in the report.

8a. CONTRACT OR GRANT NUMBER: If appropriate, enter the applicable number of the contract or grant under which the report was written.

8b, 8c, & 8d. PROJECT NUMBER: Enter the appropriate military department identification, such as project number, subproject number, system numbers, task number, etc.

9a. ORIGINATOR'S REPORT NUMBER(S): Enter the official report number by which the document will be identified and controlled by the originating activity. This number must be unique to this report.

9b. OTHER REPORT NUMBER(S): If the report has been assigned any other report numbers *(either by the originator or by the sponsor)*, also enter this number(s).

10. AVAILABILITY/LIMITATION NOTICES: Enter any limitations on further dissemination of the report, other than those imposed by security classification, using standard statements such as:

(1) "Qualified requesters may obtain copies of this report from DDC."

(2) "Foreign announcement and dissemination of this report by DDC is not authorized."

(3) "U. S. Government agencies may obtain copies of this report directly from DDC. Other qualified DDC users shall request through _____."

(4) "U. S. military agencies may obtain copies of this report directly from DDC. Other qualified users shall request through _____."

(5) "All distribution of this report is controlled. Qualified DDC users shall request through _____."

If the report has been furnished to the Office of Technical Services, Department of Commerce, for sale to the public, indicate this fact and enter the price, if known.

11. SUPPLEMENTARY NOTES: Use for additional explanatory notes.

12. SPONSORING MILITARY ACTIVITY: Enter the name of the departmental project office or laboratory sponsoring *(paying for)* the research and development. Include address.

13. ABSTRACT: Enter an abstract giving a brief and factual summary of the document indicative of the report, even though it may also appear elsewhere in the body of the technical report. If additional space is required, a continuation sheet shall be attached.

It is highly desirable that the abstract of classified reports be unclassified. Each paragraph of the abstract shall end with an indication of the military security classification of the information in the paragraph, represented as *(TS), (S), (C), or (U).*

There is no limitation on the length of the abstract. However, the suggested length is from 150 to 225 words.

14. KEY WORDS: Key words are technically meaningful terms or short phrases that characterize a report and may be used as index entries for cataloging the report. Key words must be selected so that no security classification is required. Identifiers, such as equipment model designation, trade name, military *project code name, geographic location, may be used as key* words but will be followed by an indication of technical context. The assignment of links, roles, and weights is optional.

ABSTRACT

A band of naturally occurring radio noise between the local electron plasma frequency and the upper hybrid resonance frequency is frequently observed by the University of Iowa plasma wave experiment on the IMP-6 satellite. This radio noise band has been observed over a large range of geocentric radial distances extending from well inside the plasmapause boundary to greater than 10 earth radii in the outer magnetosphere. The center frequency of the noise band decreases systematically with increasing radial distance and changes abruptly at the plasmapause boundary, typically from about 100 kHz just inside the plasmapause to about 10 to 30 kHz outside of the plasmapause. The broadband electric field strength of this noise is very small, seldom exceeding 10 microvolts $(\text{meter})^{-1}$, and probably could not be detected without using long electric antennas of the type used on IMP-6.

Because of the association of this noise band with the upper hybrid resonance frequency and the similarity to previous observations at much lower altitudes in the ionosphere we have called this noise "upper hybrid resonance noise" to be consistent with previous terminology. It is believed that this noise is produced by incoherent Cerenkov emission from super-thermal electrons. Since the cutoff frequencies of the upper hybrid resonance noise band can be measured very accurately and since the characteristic frequencies of the

ambient plasma are expected to be almost completely unaffected by the presence of the satellite it is possible to obtain very accurate (few percent) and reliable electron density measurements from the cutoff frequencies of this noise. Electron densities as low as 0.1 cm^{-3} have been measured in the region outside of the plasmapause with this technique.

In some cases a second very narrow noise band has been observed at a frequency slightly above the second harmonic of the electron gyrofrequency. This noise band is thought to be associated with the electrostatic Bernstein mode which occurs at frequencies near the second harmonic of the electron gyrofrequency.

I. INTRODUCTION

Naturally occurring radio noise at frequencies greater than the electron plasma frequency and less than the upper hybrid resonance frequency has been observed at relatively low altitudes in the ionosphere by several rocket- and spacecraft-borne radio noise experiments [Walsh et al., 1964; Bauer and Stone, 1968; Muldrew, 1970; Hartz, 1970; and Gregory, 1969]. Since the index of refraction for the extraordinary mode of propagation near the upper hybrid resonance is greater than one, it is generally believed that this noise is produced by Cerenkov radiation from super-thermal electrons. The University of Iowa plasma wave experiment on the IMP-6 spacecraft has detected a similar noise band believed to be associated with the upper hybrid resonance frequency at large radial distances in the magnetosphere. This noise band extends downward from the local upper hybrid resonance frequency to the plasma frequency and occurs over a range of geocentric radial distances extending from well inside the plasmapause boundary to greater than 10 earth radii in the outer magnetosphere.

A second narrow band of noise has also been observed to occur slightly above the second harmonic of the electron gyrofrequency. This noise band is believed to be associated with an electrostatic Bernstein mode. Bernstein mode resonances as well as resonances at the plasma frequency and upper hybrid resonance frequency have been detected

in the ionosphere by topside sounders [Knecht, et al., 1961; Calvert and Goe, 1963; and Lockwood, 1963].

The purpose of this paper is to describe the upper hybrid resonance noise bands detected by the IMP-6 plasma wave experiment, to discuss the physical origin of the noise, and to present typical magnetospheric electron density profiles obtained from the cutoff frequency of these noise bands.

II. DESCRIPTION OF INSTRUMENTATION

The IMP-6 spacecraft was launched on March 13, 1971, into a highly eccentric earth orbit with initial perigee and apogee geocentric radial distances of 6613 km and 212,630 km, respectively, orbit inclination of 28.7 degrees, and period of 4.18 days. This orbit carries IMP-6 through the plasmasphere, magnetosheath, bow shock and into the solar wind. IMP-6 is a spin stabilized spacecraft with the spin axis oriented nearly perpendicular to the ecliptic plane and a nominal rotation period of about 11 seconds.

The University of Iowa plasma wave experiment on IMP-6 detects plasma wave phenomena in the frequency range from 20 Hz to 200 kHz. The antennas for this experiment consist of three mutually orthogonal "long-wire" dipole antennas for electric field measurements and three mutually orthogonal loop antennas for magnetic field measurements. Two of the electric dipole antennas are perpendicular to the spacecraft spin axis. These antennas, E_x and E_y, have tip-to-tip lengths of 53.5 meters and 92.5 meters respectively. The E_z antenna which lies along the spin axis has a tip-to-tip length of 7.7 meters. Any of the six antennas may be connected to either of two identical spectrum analyzers and two wideband receivers.

Each of the two spectrum analyzers consists of sixteen channels with center frequencies from 35 Hz to 178 kHz. The filter for each

channel has a bandwidth of approximately fifteen percent of the center frequency and there are four filters per decade of frequency. Each frequency channel has two detectors, a peak detector and an average detector. The peak detector has a response time constant of 0.1 seconds and measures the largest signal occurring in a given sample interval (5.11 seconds), and the average detector measures the average noise intensity, with a time constant of 5.11 seconds, during each sample interval. In addition to the peak and average detectors the 35 Hz, 311 Hz, 3.11 kHz, and 31.1 kHz channels also have a rapid sample detector output. The time constant of this detector is 0.1 seconds and it is sampled every 0.32 seconds. The telemetered output of each detector is a voltage proportional to the logarithm of the quantity being measured. The dynamic range of each spectrum analyzer channel is 100 db.

The spectrum analyzer channels each have an r.m.s. sensitivity of about 10 microvolts for a sine wave signal. When connected to one of the long electric dipole antennas, this sensitivity permits measurements of electric field strengths as low as 0.2 microvolts $(\text{meter})^{-1}$. The corresponding magnetic field sensitivity of the loop antenna is a function of frequency and varies from about 2.0 milligammas at 35 Hz to about 10.0 microgammas at 16.5 kHz.

In conjunction with the two spectrum analyzers, the University of Iowa plasma wave experiment includes two wideband receivers. These receivers are automatic gain control receivers and provide broadband coverage of the frequency ranges from 10 Hz to 1 kHz and from 650 Hz

to 30 kHz, depending on the particular mode of operation selected. The analog signals from the wideband receivers are transmitted to the ground via the special purpose analog transmitter. These wideband signals are used for high frequency-time resolution analysis of transient and narrow band wave phenomena.

III. CHARACTERISTICS OF UPPER HYBRID RESONANCE NOISE OBSERVED BY IMP-6

The spectrum analyzer data for an outbound IMP-6 pass through the magnetosphere, from about 2.0 to 10.0 earth radii geocentric radial distance, are shown in Figure 1. The data on the left side of the figure are the raw voltage outputs of the two spectrum analyzers, one of which is connected to an electric dipole antenna (E_y) and the other of which is connected to a magnetic loop (B_y) antenna. The vertical bars for each of the sixteen frequency channels represents the average electric (or magnetic) field strength over a time interval of 81.8 seconds. The upper dotted line in each frequency channel is the largest peak field strength seen over the same time interval. The ordinate for each frequency channel is proportional to the logarithm of the electric (or magnetic) field strength. The interval from the baseline of one channel to the baseline of the next higher channel represents a dynamic range of 100 db. The enhanced signal strength in the three lowest frequency channels of the electric field spectrum analyzer starting at about 0302 UT is caused by voltage transients on the spacecraft solar array produced as the shadow of the loop antenna passes over the solar cells. The magnitude of this interference depends on several factors, the most important of which is the electron density. This dependence provides a useful method of identifying the plasmapause

boundary from the abrupt increase in the interference level as the spacecraft passes from the high density region inside the plasmasphere to the low density region outside. The abrupt increase in the low frequency electric field interference level at about 0302 UT provides a clear indication that the spacecraft crossed the plasmapause at this time.

Further evidence supporting this identification of the plasmapause location is provided by the abrupt termination of plasmaspheric hiss evident in the magnetic loop antenna data from about 200 Hz to 3 kHz. Russell et al., [1969] and Russell and Holzer [1970] have shown that this noise is usually confined to the region interior to the plasmasphere and that the outward termination of the plasmaspheric hiss corresponds closely with the plasmapause location.

A clearly defined noise band can be seen in the electric field spectrum analyzer data in the upper left panel of Figure 1 beginning at about 0220 UT in the 178 kHz channel. As the spacecraft proceeds outward to larger radial distances, the center frequency of this noise band sweeps rapidly downward through the 100 kHz, 56.2 kHz, and 31.1 kHz channels and ends its downward sweep in the 16.5 kHz and 10 kHz channels. This noise band is shown with better time resolution in the right panel of Figure 1. The time resolution for these data is 5.11 seconds and absolute electric field spectral densities are given for each channel. These spectral densities have been computed by assuming that the effective length of the electric antenna is one half of the tip-to-tip length and that the antenna impedance is small compared to the base

loading impedance. Although these assumptions are believed to be valid under most conditions, it is possible that significant errors could occur if the antenna impedance becomes significantly larger than the free space impedance.

The abrupt decrease in the center frequency of the noise band shown in Figure 1, from ~ 100 kHz at 0258 UT to ~ 31.1 kHz at 0308 UT, is seen to correspond closely with the location of the plasmapause. Because of the distinctive frequency variation at the plasmapause boundary, decreasing in frequency with the decrease in electron density at the plasmapause boundary, and the qualitative similarity to upper hybrid resonance noise observations at lower altitudes in the ionosphere we believe that this noise band is associated with the upper hybrid resonance frequency,

$$f_{UHR} = \sqrt{f_p^2 + f_g^2} \quad , \qquad (1)$$

where f_p is the electron plasma frequency (proportional to the square root of the electron density) and f_g is the electron gyrofrequency [see Stix, 1962]. Quantitative considerations also show that this identification is reasonable.

Another outgoing IMP-6 pass which clearly shows an upper hybrid resonance noise band is illustrated in Figure 2. The abrupt decrease in the frequency of the noise band at the plasmapause boundary is again evident. Similar noise bands can be identified on approximately two-thirds of the IMP-6 passes through the magnetosphere. Because the

B

intensity of this noise is so small, typically only 3.0 microvolts $(\text{meter})^{-1}$ broadband electric field strength, this noise band is clearly distinguishable only during "quiet" times for which other magnetospheric radio emissions occurring in this frequency range are undetectable. During sufficiently quiet periods it is always possible to identify the upper hybrid resonance noise band, indicating that this noise is an essentially permanent feature of the outer magnetosphere. Upper hybrid resonance noise has been observed at essentially all local times and at radial distances from 3.0 earth radii to about 10.0 earth radii. The lower radial distance limit (3.0 earth radii) for these observations occurs because the center frequency of the noise band goes above the highest frequency channel of the spectrum analyzer. This limit is not, therefore, an actual limit on the region of occurrence of the noise. At large radial distances the upper hybrid resonance noise band always disappears at the magnetopause boundary and is generally very difficult to clearly identify at radial distances greater than about 10.0 earth radii. In no case has it been possible to detect the upper hybrid resonance noise with the magnetic loop antenna.

Much higher resolution frequency-time spectrums of these noise bands can be obtained at frequencies below 30 kHz from the wideband analog telemetry. Figure 3 shows a high resolution frequency-time spectrogram of the upper hybrid resonance noise illustrated in Figure 2 at about 1613 UT. The IMP-6 wideband receiver filters the detected electric and magnetic field signals into three frequency ranges (1) 650 Hz - 10 kHz, (2) 10 kHz - 19.35 kHz, and (3) 20.65 kHz - 30 kHz.

These frequency ranges are then sequentially switched every 40.91 seconds and transmitted to the ground in a single 650 Hz to 10 kHz frequency band. The data shown in Figure 3 represent one 40.91 second interval from the 10 kHz - 19.35 kHz band followed by a similar interval from the 20.65 kHz - 30 kHz band. The frequency scales of these spectrograms have been appropriately displaced to provide a linear frequency scale from 10 kHz to 30 kHz. The wideband receiver is alternately connected to the magnetic, B_y, and the electric, E_x, antennas for the first and second half of each 40.91 second interval.

The upper hybrid resonance noise band is clearly evident in the electric field spectrograms of Figure 3 in the frequency range from about 12.0 kHz to 16.0 kHz. The noise band is not detectable with the magnetic loop antenna. Sharp nulls are evident in the electric field data at twice the spacecraft spin rate. As indicated in Figure 3, these nulls occur when the electric antenna axis is parallel to the geomagnetic field. The geomagnetic field vector in this case is very nearly perpendicular to the spacecraft spin (z) axis so that the electric antenna axis is approximately parallel to the geomagnetic field twice per rotation. The geomagnetic field measurements were made simultaneously by the NASA/GSFC magnetometer on IMP-6 and were provided by Dr. N. F. Ness [personal communication, 1972]. This spin modulation indicates that the electric field vector of the noise is oriented very nearly perpendicular to the geomagnetic field.

Several previous rocket and satellite observations of upper hybrid resonance noise at lower altitudes in the ionosphere have shown

that the upper cutoff frequency of the noise band corresponds to the upper hybrid resonance frequency of the local plasma. As indicated in Figure 2, we have therefore assumed that the upper cutoff frequency of the noise band is the upper hybrid resonance frequency, f_{UHR}, of the local plasma. Since the electron gyrofrequency, f_g, can be determined from the measured magnetic field the electron plasma frequency, f_p, can be calculated directly from Equation 1. The electron plasma frequency, f_p, thus determined, is indicated in Figure 3. It is evident that in this case the lower cutoff frequency of the noise band corresponds closely with the electron plasma frequency.

A series of spectrograms obtained on another IMP-6 pass through the outer magnetosphere is shown in Figure 4. An upper hybrid resonance noise band is clearly evident in these spectrograms, increasing in frequency as the spacecraft proceeds to smaller geocentric radial distances. Again the noise band extends downward from the upper hybrid resonance frequency, f_{UHR}, to the electron plasma frequency, f_p. In this case, however, the most intense part of the noise band occurs just below the upper hybrid resonance frequency, and for a substantial portion of the pass the noise intensity in the lower portion of the band is so weak that the cutoff at the plasma frequency cannot be detected.

The spin modulation evident in Figure 4 shows that the electric field in the most intense portion of the band, near the upper hybrid resonance frequency, is again perpendicular to the geomagnetic field. The spin modulation in the lower part of the band is however shifted by 90°, indicating that near the electron plasma frequency the electric field vector is parallel to the geomagnetic field. A narrow band of

enhanced electric field noise is also clearly evident at the low frequency cutoff of the upper hybrid resonance noise band in the 1625:20 to 1625:50 UT spectrogram of Figure 4. Since the frequency of this narrow band of noise is very close to the computed electron plasma frequency, we believe that this noise is caused by electrostatic plasma oscillations at the local electron plasma frequency. The spin modulation of this noise shows that the electric field is parallel to the geomagnetic field as would be expected for an electrostatic electron plasma oscillation.

Another type of noise band, not directly related to the upper hybrid resonance noise, but often occuring at comparable frequencies in the same region of space, is also frequently observed with IMP-6. An example of this noise can be seen at a frequency of about 21 kHz in Figure 3. This noise band occurs at a frequency of 2.22 f_g and is very narrow and weak, less than 1 microvolt $(\text{meter})^{-1}$. We believe that this noise band is associated with the electrostatic Bernstein mode [Bernstein, 1958] near the second harmonic of the electron gyrofrequency. Crawford, Harp, and Mantei [1967] have computed the dispersion relation for this mode of propagation. The dispersion relation predicts that propagation is possible for wave frequencies in a band extending from a given integral multiple of the electron gyrofrequency to a frequency slightly higher than that particular multiple of the gyrofrequency. Dougherty and Monaghan [1965] have derived an approximate formula for the highest frequency which can propagate in a band near a multiple of the electron gyrofrequency. For the second harmonic of the gyrofrequency their approximation gives

$$\frac{f}{f_g} = 2\left[1 + \left(\frac{f_p}{f_g}\right)^2 F(\eta)\right]$$

$$F(\eta) = \frac{e^{-\eta} I_2(\eta)}{\eta}$$

where $\eta = (k_\perp R_{th})^2$, $k_\perp$ is the wave number perpendicular to the geomagnetic field, R_{th} is the mean electron gyro-radius, and $I_2(\eta)$ is the modified Bessol function of order two. The function $F(\eta)$ has a maximum value of $F(\eta) \simeq 0.0509$ at $\eta \simeq 1.25$. Using this maximum value for $F(\eta)$ and the plasma frequency and gyrofrequency shown in Figure 3, the upper frequency limit of the Bernstein mode is computed to be $f = 2.16\ f_g$. As can be seen in Figure 3, the noise band has a sharp upper cutoff frequency at $f = 2.22\ f_g$ with the noise fading out gradually below this frequency. The computed upper frequency limit for the Bernstein mode, $f = 2.16\ f_g$, is within 3% of the measured upper cutoff frequency of $f = 2.22\ f_g$. As can also be seen from the spin modulation of this noise band, the wave electric field is perpendicular to the geomagnetic field and there is no detectable wave magnetic field, as would be expected for the Bernstein mode. Thus we conclude that this noise band is associated with the electrostatic Bernstein mode near the second harmonic of the electron gyrofrequency.

IV. THE THEORY OF UPPER HYBRID RESONANCE NOISE

In order to provide a basis for interpreting the upper hybrid resonance noise observations of IMP-6 we will consider a simple model of wave propagation in a cold plasma at frequencies near the upper hybrid resonance frequency. Figure 5 shows a radial profile of the relevant cutoff and resonance frequencies for a dayside magnetospheric model. The characteristic frequencies shown, using the notation of Stix [1962], are the R=0 cutoff frequency, $f_{R=0}$; the upper hybrid resonance frequency, f_{UHR}, the plasma frequency, f_p, and the L=0 cutoff frequency, $f_{L=0}$. The CMA diagram for a single component plasma is also shown at the top of Figure 5 in terms of the normalized parameters.

$$X = \left(\frac{f_p}{f}\right)^2 \text{, and } Y = \left(\frac{f_g}{f}\right),$$

commonly used in magneto-ionic theory [Ratcliff, 1962]. Because the upper hybrid resonance noise is observed within only a limited range of radial distances at any given frequency, it is concluded that this noise must correspond to the extraordinary mode of propagation which exists between the upper hybrid resonance frequency and the L=0 cutoff frequency. The region of propagation for this mode is shown by the crosshatching in Figure 5. Note that this mode of propagation is completely trapped within the magnetosphere and cannot escape.

In the frequency range between the upper hybrid resonance frequency and the maximum of either the plasma frequency or the electron gyrofrequency the index of refraction goes to infinity at the resonance cone angle θ_R, relative to the geomagnetic field, given by

$$\mathrm{Tan}^2\ \theta_R = -\frac{P}{S}\ .$$

The region within which this resonance in the refractive index occurs is shown by the double crosshatching in Figure 5. The resonance cone angle θ_R varies from zero degrees at the plasma frequency to ninety degrees at the upper hybrid resonance frequency, above which the mode does not propagate. The index of refraction is less than one for all angles below the plasma frequency and goes to zero at the L=0 cutoff frequency. Extraordinary mode waves are therefore reflected away from the L=0 boundary.

Because the index of refraction for the extraordinary mode becomes very large in the region where a resonance cone exists, Cerenkov radiation can be produced by super-thermal charged particles in this region. In order to determine what happens to extraordinary mode waves which are generated by Cerenkov radiation in this region, we have investigated the propagation of this mode using the plane stratified model shown in Figure 6. If the plasma parameters, electron density and magnetic field, vary primarily in the direction normal to the planes of constant f_p and f_{UHR}, then the component of the index of refraction vector parallel to the planes of stratification is a

constant (Snell's Law). The group velocity $\vec{V}_g$ and the ray path can then be determined from the refractive index surface by a simple geometric construction as illustrated in Figure 6. The plane startified model is expected to be a good approximation near the magnetic equator and in other regions when the distance between the $f = f_{UHR}$ and $f = f_p$ surfaces is small compared to the scale length for magnetic field variations. A similar plane stratified model has been used previously by McAfee [1969] to calculate ray paths near the upper hybrid resonance frequency in the ionosphere.

An example of a wave emitted by a 5 keV electron at a frequency equal to 1.17 f_p is shown in Figure 6. The initial wave normal direction, θ_c, of the emitted Cerenkov radiation can be found by a graphical solution of the Cerenkov condition [Jorgensen, 1968],

$$n(\theta_c) = \frac{c}{v_{||}} \text{Cos } \theta_c \ ,$$

where $n(\theta_c)$ is the refractive index, and $v_{||}$ is the component of the electron velocity parallel to the geomagnetic field (see Figure 6). Once emitted the component of the index of refraction parallel to the surfaces of constant f_{UHR} and f_p is conserved, as indicated by the vertical dashed lines in Figure 6.

Both upgoing and downgoing waves are emitted by Cerenkov radiation. Because the resonance cone angle goes to ninety degrees at $f = f_{UHR}$, the ray path for the upgoing wave is refracted away from the $f = f_{UHR}$ surface and becomes asymptotically parallel to this

surface as resonance occurs. At resonance, which always occurs somewhat below the $f = f_{UHR}$ surface, the wave is absorbed by the plasma, due to either collisions or thermal (Landau) damping. For the case illustrated in Figure 6 resonance occurs when $f \sim 1.24\ f_p$ ($f_{UHR} = 1.25\ f_p$).

The downgoing wave will be able to cross the $f = f_p$ surface only if the component of the index of refraction parallel to the plane of stratification is less than one since the index of refraction below the plasma frequency is less than one. Because the major contribution to the Cerenkov radiation comes from electrons with $v_{||} \ll c$, the emitted waves have a large index of refraction and the downgoing waves generally cannot cross the $f = f_p$ surface. Downgoing waves are then reflected at the $f = f_p$ surface, similar to the "Spitze" reflection encountered in ionospheric sounding [Budden, 1961], or somewhat above the $f = f_p$ surface if wave vector directions out of the plane of the paper are considered. Downgoing waves can propagate past the $f = f_p$ surface only if the geomagnetic field makes a large angle relative to the $f = f_p$ surface, as could occur at very high geomagnetic latitudes, or if the Cerenkov radiation is produced by very energetic (relativistic) electrons. Any downgoing waves which do succeed in crossing the $f = f_p$ surface in this manner are reflected as they approach the $f_{L=0}$ cutoff (see Figure 5).

As the Cerenkov radiation propagates toward either the $f = f_p$ or $f = f_{UHR}$ surfaces the relative magnitudes of the wave electric and magnetic fields change in value. Near the $f = f_{UHR}$ surface the component of the wave electric field perpendicular to the geomagnetic

field becomes large compared to the other components and the wave becomes electrostatic. Likewise, near the $f = f_p$ surface the component of the wave electric field parallel to the geomagnetic field becomes large relative to the perpendicular component. Because the index of refraction is usually much greater than one in this region the electric field energy is usually much larger than the magnetic field energy.

Discussion

This qualitative analysis of the Cerenkov radiation generated near the upper hybrid resonance frequency indicates that this radiation should exhibit the following characteristics:

(1) The radiation should be primarily trapped in the frequency range $f_{UHR} > f > f_p$ and only under special conditions should the radiation be able to reach the frequency range $f_p > f > f_{L=0}$.

(2) The frequency spectrum of the radiation should be broad-band since it is generated by an incoherent process.

(3) Near the upper hybrid resonance frequency the wave electric field should be nearly perpendicular to the geomagnetic field.

(4) Near the plasma frequency the wave electric field should be nearly parallel to the geomagnetic field.

(5) The electric field energy density generally should be much larger than the magnetic field energy density.

The upper hybrid resonance noise observed by IMP-6 fits these characteristics very well. In all cases investigated the noise is

clearly confined to the frequency range $f_p < f < f_{UHR}$. In many cases both the upper cutoff at f_{UHR} and the lower cutoff at f_p can be detected and the measured cutoff frequencies typically agree to within a few percent of the calculated cutoffs. In no case has noise been detected in the frequency range $f_{L=0} < f < f_p$, although Mosier et al. [1973] have observed noise in this frequency range at lower altitudes within the plasmasphere and their observations show that the noise intensities below the plasma frequency are significantly attenuated relative to the intensities above the plasma frequency, as would be expected if only a small fraction of the Cerenkov radiation can reach this region. Within the frequency range $f_p < f < f_{UHR}$ the noise intensity varies significantly, usually with the largest intensity near the upper hybrid resonance frequency. Since the upgoing ray paths become asymptotic to the $f = f_{UHR}$ surface near the upper hybrid resonance, the largest intensities are expected near the upper hybrid resonance frequency, although the exact spectrum depends in detail on the electron energy spectrum, the magnetic field direction and other complicating factors. The example shown in Figure 4, as well as several other cases studied, shows the expected variation in the electric field direction, from perpendicular to the geomagnetic field near the upper hybrid resonance to parallel to the geomagnetic field near the plasma frequency. In no case has a wave magnetic field been detected for the upper hybrid resonance noise, although this is mainly attributed to the lower sensitivity of the magnetic loop antenna compared to the electric dipole antenna.

Calculations by Muldrew [1970] indicate that incoherent Cerenkov radiation generates sufficient power to be the source of upper hybrid resonance noise observed in the ionosphere. Calculations by Taylor and Shawhan [1973] estimating the total electric field spectral density in the extraordinary mode caused by Cerenkov emission, indicate that incoherent Cerenkov radiation can explain the electric field intensity of the upper hybrid resonance noise observed by IMP-6.

V. ELECTRON DENSITY PROFILES OBTAINED FROM UPPER HYBRID RESONANCE NOISE

Bauer and Stone [1968] used observations of upper hybrid resonance noise made by the radio astronomy experiment on ATS II to measure the electron density out to radial distances of 2 R_E. The upper hybrid resonance noise observed by IMP-6 can be used to determine electron density profiles at radial distances greater than 3 R_E. Figures 7 and 8 show two examples of electron number density profiles obtained from upper hybrid resonance noise measurements and from simultaneous geomagnetic field measurements made by the NASA/GSFC magnetometer experiment on IMP-6. Figures 7 and 8 clearly show the plasmapause boundary between L = 4 and L = 5, and the decreasing electron number density out the several earth radii beyond the plasmapause. The largest four number density values in both figures were calculated using data from the upper four spectrum analyzer channels and the remaining values were obtained using spectrum measurements from the wideband receivers. Both sets of data were taken during relatively quiet geomagnetic activity, and somewhat different latitudes and local times.

The upper hybrid resonance noise band used to calculate the number density profiles shown in Figures 7 and 8 were chosen to extend over the entire interval from $f_p < f < f_{UHR}$. Independent measurements of the upper and lower frequency limits of the noise band were taken

and the electron density was calculated by two methods: (1) by setting the lower frequency limit equal to the plasma frequency and (2) by setting the upper frequency limit equal to the upper hybrid resonance frequency. As shown in Figures 7 and 8, the electron densities obtained from both methods are in excellent agreement.

Accurate electron number density measurements to values as low as a few tenths of a particle per cubic centimeter may be obtained from the upper hybrid resonance noise data. These profiles are in excellent agreement with the number density measurements made by the light ion mass spectrometer on OGO-5 [Harris, et al., 1970 and Chappell, et al., 1971]. The H+ ion concentrations measured by Harris et al. have typical values between 1 cm^{-3} and 0.1 cm^{-3} outside the plasmapause. The upper hybrid resonance measurements are, however, believed to be considerably more accurate than the plasma probe electron density measurements. There are several factors which may produce significant errors in the ion concentrations measured by direct plasma probe measurements. According to Harris, et al., the H+ ion concentrations may be underestimated by as much as 40% due to the motion of the spacecraft through the plasma. Also, positive spacecraft potentials may cause focusing of thermal ions into the spectrometer entrance which cannot be easily corrected. The plasma wave measurements, however, suffer none of the problems caused by perturbations of the plasma by the spacecraft. As long as the waves observed have a spatial extent much greater than the spacecraft dimensions local effects do not cause errors in the observed frequency spectrum. It is possible that Doppler shifts could cause

errors in the measured frequencies, however, Doppler shifts are not believed to be significant for the upper hybrid resonance noise. Spin modulation of the upper cutoff frequency should be observed if Doppler shifts are important. As the antenna rotates, the antenna pattern selects wave vectors which have different orientation with respect to the velocity vector of the spacecraft and, therefore, different Doppler shifts. Such spin modulation can be seen for lower hybrid resonance noise observed by INJUN 5 [Gurnett et al., 1969]. However, no such spin modulation has been identified at the upper cutoff of the upper hybrid resonance noise band observed by IMP-6. Doppler shifts are, therefore, thought to be a negligible source of error in these measurements. Another possible source of error in determination of the upper hybrid resonance frequency could arise if the wavelengths of the waves at the resonance frequency become shorter than the antenna length. The upper hybrid resonance frequency would then lie slightly higher than the highest frequency observed in the noise band because the antenna would not detect the short wave lengths occurring near the resonance. This type of error does not appear to be significant as is evidenced by the consistency in calculated number densities using both the measured upper and lower limits of the noise bands as shown in Figure 7 and 8. We have estimated that the maximum error in measuring the cutoff frequencies of the upper hybrid resonance noise band is $\pm$250 Hz. This error in measuring the cutoff frequencies is considered quite conservative and typically results in an uncertainty of about 3% in the computed electron density.

The plasma wave measurements made in this region have produced an independent, highly accurate technique for determining the electron number density in the region beyond the plasmapause boundary. The technique is nearly independent of any parameters introduced by the presence of the spacecraft in the medium and is believed to be more accurate than any technique previously used for measuring the low electron concentrations found in the outer magnetosphere.

ACKNOWLEDGMENTS

We thank Dr. Norman F. Ness of the Goddard Space Flight Center for providing us with the geomagnetic field strengths as measured by the NASA/GSFC magnetometer experiment on IMP-6.

This work was supported in part by the National Aeronautics and Space Administration under Contract NAS5-11704 and Grant NGL-16-001-043 and by the Office of Naval Research under Grant N00014-68-A-0196-0003.

REFERENCES

Bauer, S. J., and R. G. Stone, Satellite observations of radio noise in the magnetosphere, Nature, 218, 1145-1147, 1968.

Bernstein, I.B., Waves in a plasma in a magnetic field, Phys. Rev., 109, 10-21, 1958.

Budden, K. G., Radio Waves in the Ionosphere, Cambridge University Press, Cambridge, 260-262, 1961.

Calvert, W., and G. B. Goe, Plasma resonances in the upper ionosphere, J. Geophys. Res., 68, 6113-6120, 1963.

Carpenter, D. L., Whistler studies of the plasmapause in the magnetosphere, 1, Temporal variations in the position of the knee and some evidence on plasma motions near the knee, J. Geophys. Res., 71, 693-709, 1966.

Chappell, C. R., K. K. Harris, and G. W. Sharp, The dayside of the plasmasphere, J. Geophys. Res., 76, 7632-7647, 1971.

Crawford, F. W., R. S. Harp, and T. D. Mantei, On the interpretation of ionospheric resonances stimulated by Allouette I, J. Geophys. Res., 72, 57-68, 1967.

Dougherty, J. P., and J. J. Monaghan, Theory of resonances observed in ionograms taken by sounders above the ionosphere, Proc. Roy. Soc., London, A289, 214-234, 1965.

Gregory, P. C., Radio emission from auroral electrons, Nature, 221, 350-352, 1969.

Gurnett, D. A., G. W. Pfeiffer, R. R. Anderson, S. R. Mosier, and D. P. Cauffman, Initial observations of VLF electric and magnetic fields with the Injun 5 satellite, J. Geophys. Res., 74, 4631-4648, 1969.

Harris, K. K., G. W. Sharp, and C. R. Chappell, Observations of the plasmapause from OGO 5, J. Geophys. Res., 75, 219-224, 1970.

Hartz, T. R., Low frequency noise emissions and their significance for energetic particle processes in the polar ionosphere, The Polar Ionosphere and Magnetospheric Processes, Gordon Breach Publishing Co., New York, 151-160, 1970.

Jorgensen, T. S., Interpretation of auroral hiss measured on OGO 2 and at Byrd Station in terms of incoherent Cerenkov radiation, J. Geophys. Res., 73, 1055-1069, 1968.

Kencht, R. W., T. E. Van Zandt, and S. Russell, First pulsed radio soundings of the topside of the ionosphere, J. Geophys. Res., 66, 3078-3081, 1961.

Lockwood, G. E., Plasma and electron spike phenomena observed in topside ionograms, Can. J. Phys., 41, 190-194, 1963.

McAfee, J. R., Topside ray trajectories near the upper hybrid resonance, J. Geophys. Res., 74, 6403-6408, 1969.

Mosier, S. R., Michael L. Kaiser, and Larry W. Brown, Observations of noise bands associated with the upper hybrid resonance by the IMP-6 radio astronomy experiment, (submitted for publication), J. Geophys. Res., 1973.

Muldrew, D. B., Preliminary results of ISIS 1 concerning electron-density variations, ionospheric resonances, and Cerenkov radiation, Space Research X, North-Holland Publishing Co., Amsterdam, Holland, 786-794, 1970.

Ratcliffe, J. A., The Magneto-ionic Theory and Its Application to the Ionosphere, Cambridge University Press, Cambridge, 5-7, 1962.

Russell, C. T., R. E. Holzer, and E. J. Smith, OGO 3 observations of ELF noise in the magnetosphere, 1. Spatial extent and frequency of occurrence, J. Geophys. Res., 74, 755-777, 1969.

Russell, C. T., R. E. Holzer, AC magnetic fields, Particles and Fields in the Magnetosphere, D. Reidel Publishing Co., Dordrecht, Holland, 195-212, 1970.

Stix, T. H., The Theory of Plasma Waves, McGraw-Hill, New York, 27-32, 1962.

Taylor, W. W. L., and S. D. Shawhan, Cerenkov emission as an explanation of UHR noise, (in preparation), 1973.

Walsh, D., F. T. Haddock, and H. F. Schulte, Cosmic radio intensities at 1.225 and 2.0 Mc measured up to an altitude of 1700 km, Space Research IV, North-Holland Publishing Co., Amsterdam, Holland, 935-959, 1964.

FIGURE CAPTIONS

Figure 1 A plot of the spectrum analyzer raw voltage outputs for a section of orbit 64. The spacecraft moves from $L \cong 3$ to $L \cong 10$. The plasmapause boundary can be identified from the abrupt termination of plasmaspheric hiss in the lower frequency magnetic channels and the increase in the low frequency electric field interference levels at 0302 UT. The upper hybrid resonance noise band is evident in the higher frequency channels of the electric field spectrum analyzer, abruptly decreasing in frequency at the plasmapause boundary. The broadband electric field strength of the upper hybrid resonance noise is about 3 μvolts $(\text{meter})^{-1}$.

Figure 2 Another example of upper hybrid resonance noise showing the abrupt change in the frequency of the noise band at the plasmapause boundary. The spectrum analyzer is connected to the electric dipole antenna.

Figure 3 A spectrogram of the upper hybrid resonance noise shown in Figure 2. The noise band in this case extends over the frequency interval from the electron plasma frequency,

f_p, to the upper hybrid resonance frequency, f_{UHR}. The electron gyrofrequency, f_g, has been calculated from the geomagnetic field strength as measured by the NASA/GSFC magnetometer experiment. The narrow band of noise at 2.22 f_g is believed to be associated with an electrostatic Bernstein mode near the second harmonic of the electron gyrofrequency. In both cases the spin modulation indicates that the electric field is perpendicular to the geomagnetic field.

Figure 4 A series of spectrograms showing the typical sharp upper cutoff at the upper hybrid resonance frequency. The noise extends downward to the electron plasma frequency for only a few minutes near 1625 UT. The spin modulation shows that the wave electric field is parallel to the geomagnetic field near the plasma frequency, and perpenidcular to the geomagnetic field near the upper hybrid resonance frequency.

Figure 5 A model of the dayside magnetosphere showing the characteristic frequencies of the plasma for propagation near the upper hybrid resonance frequency. The crosshatched region is the extraordinary mode trapped between the upper hybrid resonance frequency f_{UHR} and the L=0 cutoff frequency $f_{L=0}$. Cerenkov radiation is expected to occur in the double crosshatched region.

Figure 6 A plane stratified model illustrating the generation and propagation of Cerenkov radiation near the upper hybrid resonance frequency. The vertical dashed lines indicate conservation of the component of the refractive index parallel to the planes of stratification (Snell's Law). The emitted radiation is reflected near $f = f_p$ and is driven into resonance upon approaching $f = f_{UHR}$. Waves can reach the region below $f = f_p$ only for a very limited range of initial wave normal directions.

Figure 7 Electron number density profile obtained from the upper hybrid resonance noise observed on orbit 7 in Figure 2. Both the upper and lower limits of the noise band, assumed to be the upper hybrid resonance frequency and the plasma frequency respectively, have been used to calculate the electron density.

Figure 8 Electron number density profile deduced from the upper hybrid resonance noise observed on orbit 51. The upper and lower limits of the noise band are taken to be the upper hybrid resonance frequency and the plasma frequency respectively.

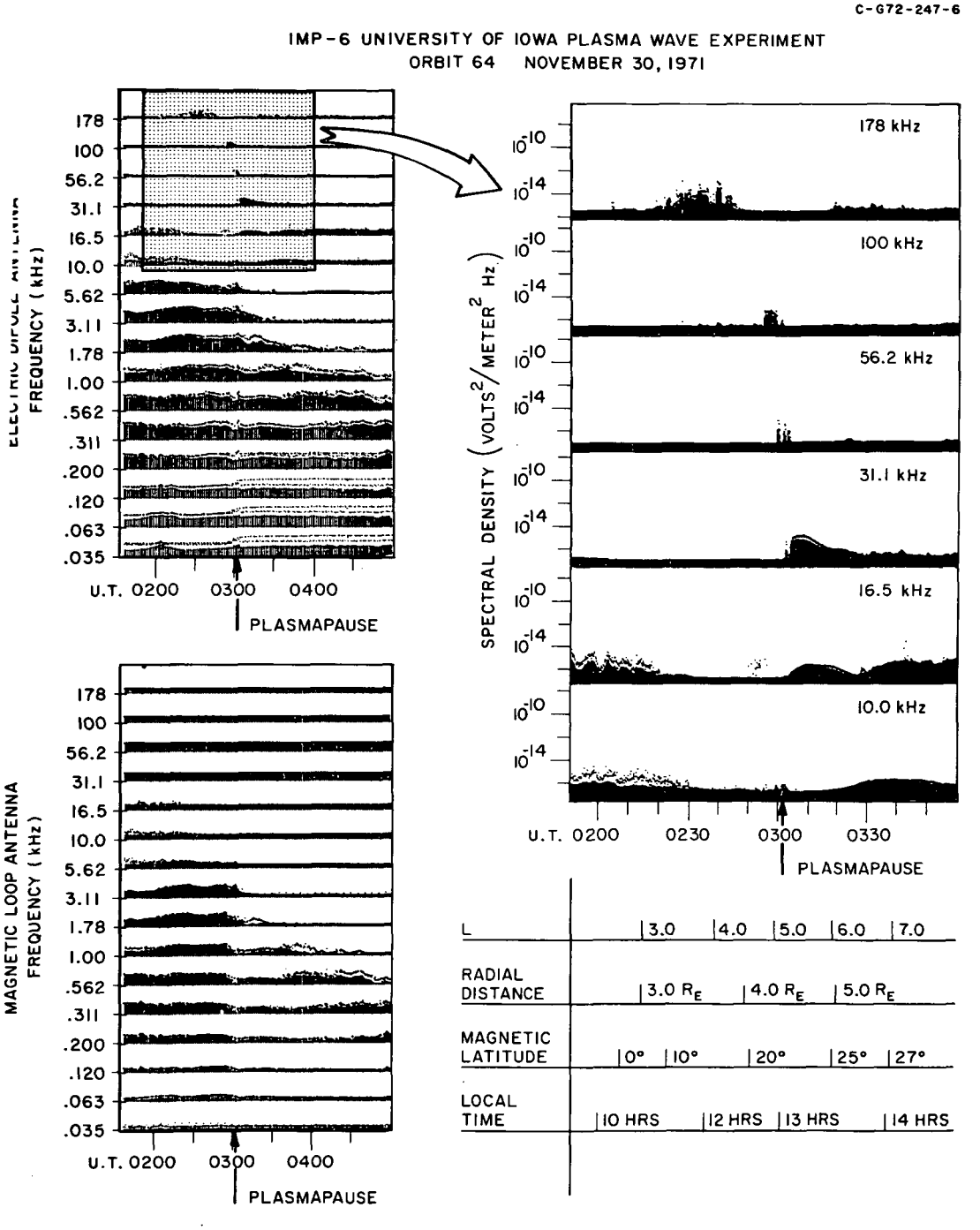
C-G72-247-6
IMP-6 UNIVERSITY OF IOWA PLASMA WAVE EXPERIMENT
ORBIT 64 NOVEMBER 30, 1971
ELECTRIC DIPOLE ANTENNA
FREQUENCY (kHz)
178
100
56.2
31.1
16.5
10.0
5.62
3.11
1.78
1.00
.562
.311
.200
.120
.063
.035
U.T. 0200
0300
0400
PLASMAPAUSE
MAGNETIC LOOP ANTENNA
FREQUENCY (kHz)
SPECTRAL DENSITY (VOLTS²/METER² Hz)
178 kHz
100 kHz
56.2 kHz
31.1 kHz
16.5 kHz
10.0 kHz
10⁻¹⁰
10⁻¹⁴
U.T. 0200
0230
0300
0330
PLASMAPAUSE
L
3.0
4.0
5.0
6.0
7.0
RADIAL DISTANCE
3.0 R_E
4.0 R_E
5.0 R_E
MAGNETIC LATITUDE
0°
10°
20°
25°
27°
LOCAL TIME
10 HRS
12 HRS
13 HRS
14 HRS

Figure 1

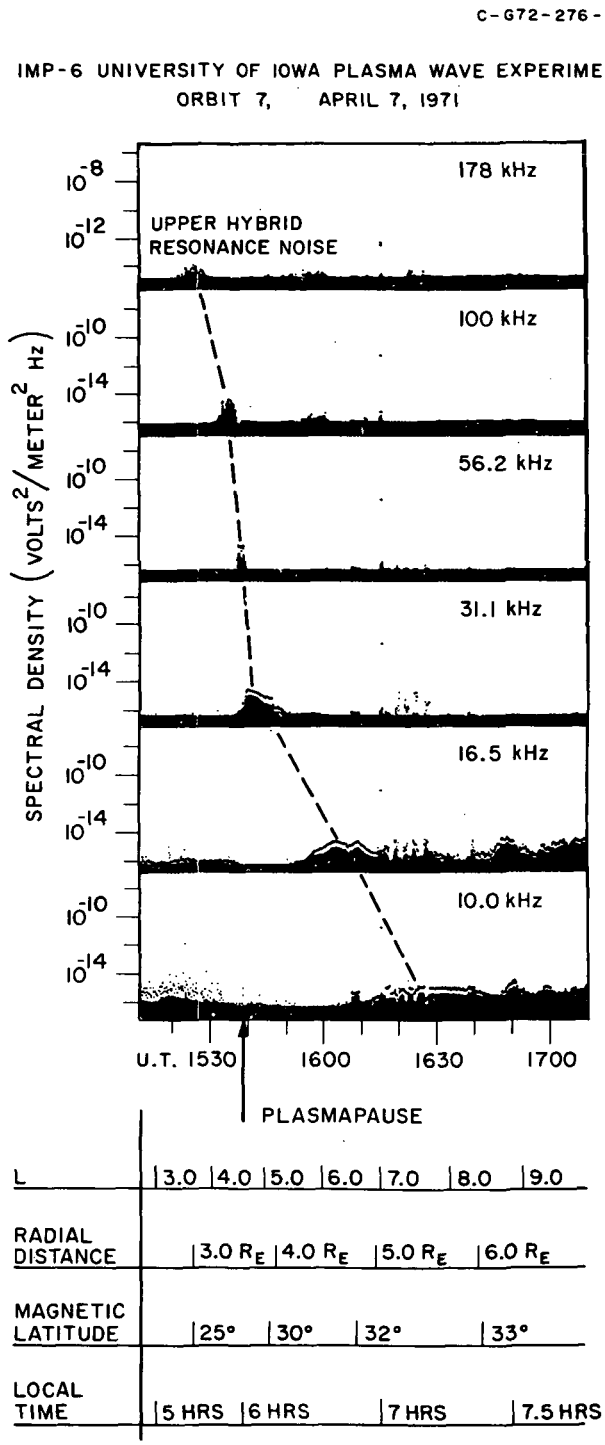
C-G72-276-2
IMP-6 UNIVERSITY OF IOWA PLASMA WAVE EXPERIMENT
ORBIT 7, APRIL 7, 1971
SPECTRAL DENSITY (VOLTS²/METER² Hz)
178 kHz
UPPER HYBRID RESONANCE NOISE
100 kHz
56.2 kHz
31.1 kHz
16.5 kHz
10.0 kHz
U.T. 1530
1600
1630
1700
PLASMAPAUSE
L
3.0 4.0 5.0 6.0 7.0 8.0 9.0
RADIAL DISTANCE
3.0 R_E 4.0 R_E 5.0 R_E 6.0 R_E
MAGNETIC LATITUDE
25° 30° 32° 33°
LOCAL TIME
5 HRS 6 HRS 7 HRS 7.5 HRS

Figure 2

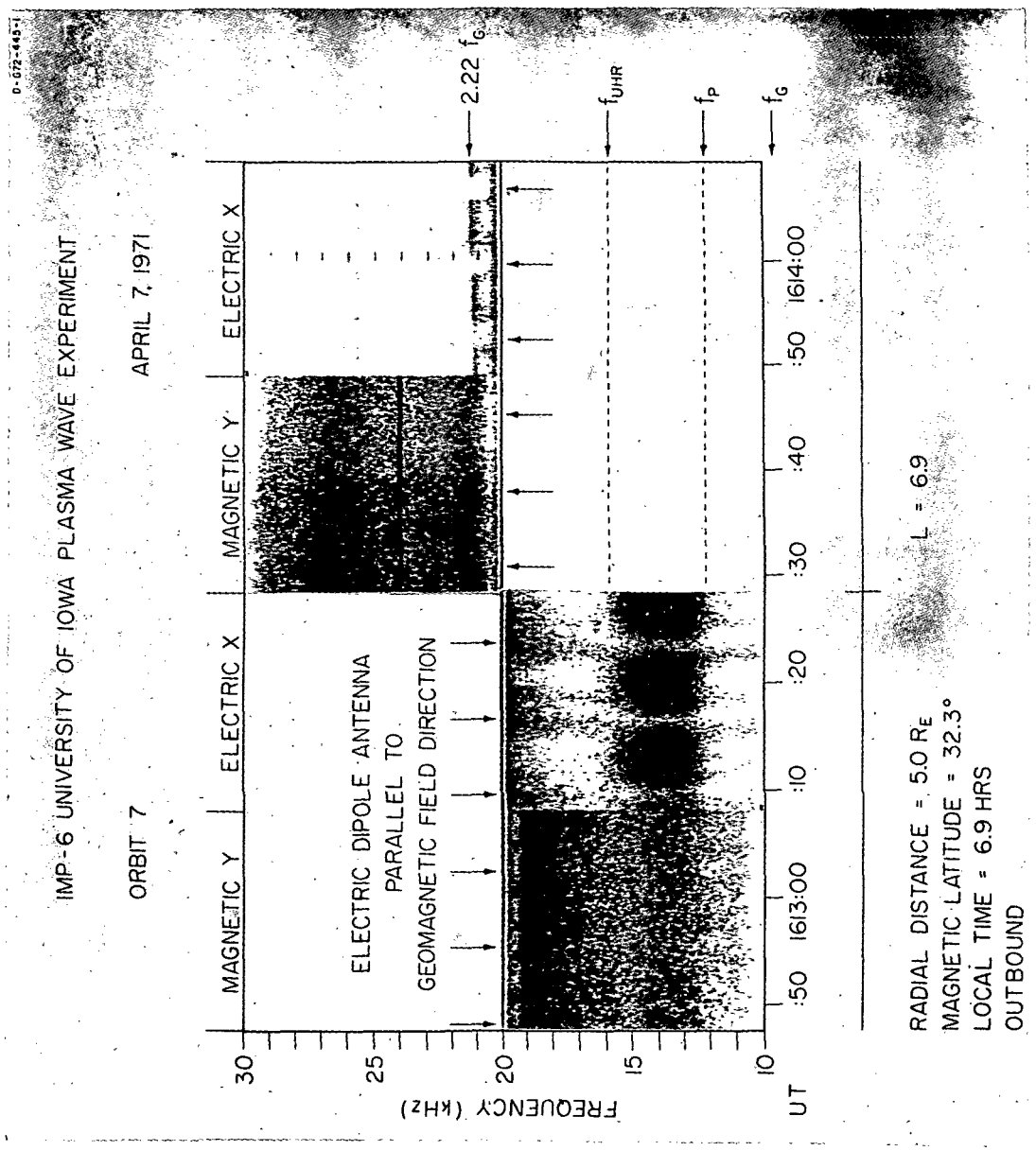
IMP-6 UNIVERSITY OF IOWA PLASMA WAVE EXPERIMENT
ORBIT 7
APRIL 7, 1971
MAGNETIC Y
ELECTRIC X
MAGNETIC Y
ELECTRIC X
ELECTRIC DIPOLE ANTENNA
PARALLEL TO
GEOMAGNETIC FIELD DIRECTION
2.22 f_G
f_{UHR}
f_P
f_G
FREQUENCY (kHz)
30
25
20
15
10
UT
:50
1613:00
:10
:20
:30
:40
:50
1614:00
RADIAL DISTANCE = 5.0 R_E
MAGNETIC LATITUDE = 32.3°
LOCAL TIME = 6.9 HRS
OUTBOUND
L = 6.9

Figure 3

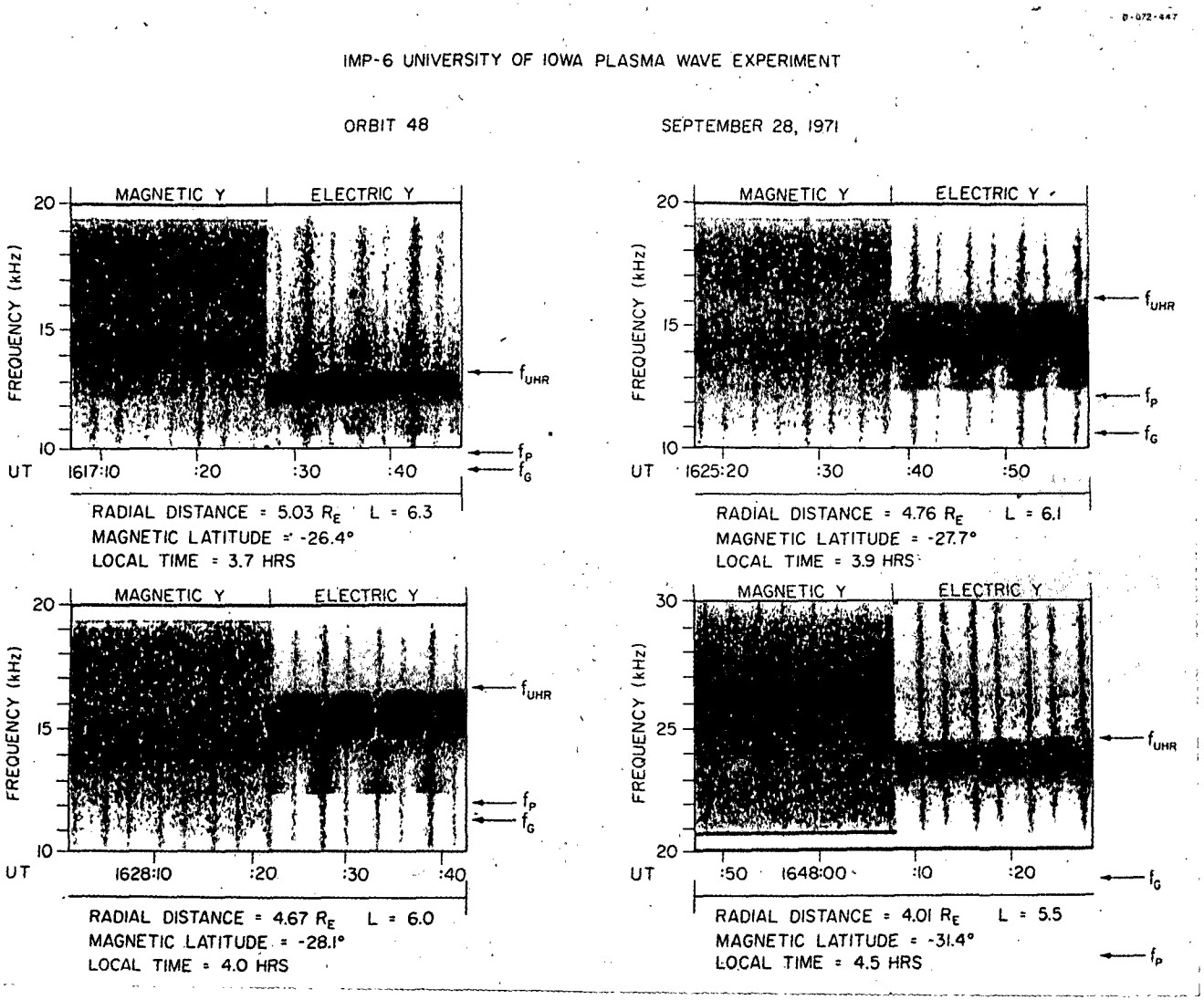
IMP-6 UNIVERSITY OF IOWA PLASMA WAVE EXPERIMENT
ORBIT 48
SEPTEMBER 28, 1971
MAGNETIC Y
ELECTRIC Y
FREQUENCY (kHz)
UT
1617:10
:20
:30
:40
f_{UHR}
f_P
f_G
RADIAL DISTANCE = 5.03 R_E L = 6.3
MAGNETIC LATITUDE = -26.4°
LOCAL TIME = 3.7 HRS
1625:20
:50
RADIAL DISTANCE = 4.76 R_E L = 6.1
MAGNETIC LATITUDE = -27.7°
LOCAL TIME = 3.9 HRS
1628:10
RADIAL DISTANCE = 4.67 R_E L = 6.0
MAGNETIC LATITUDE = -28.1°
LOCAL TIME = 4.0 HRS
1648:00
:10
RADIAL DISTANCE = 4.01 R_E L = 5.5
MAGNETIC LATITUDE = -31.4°
LOCAL TIME = 4.5 HRS

Figure 4

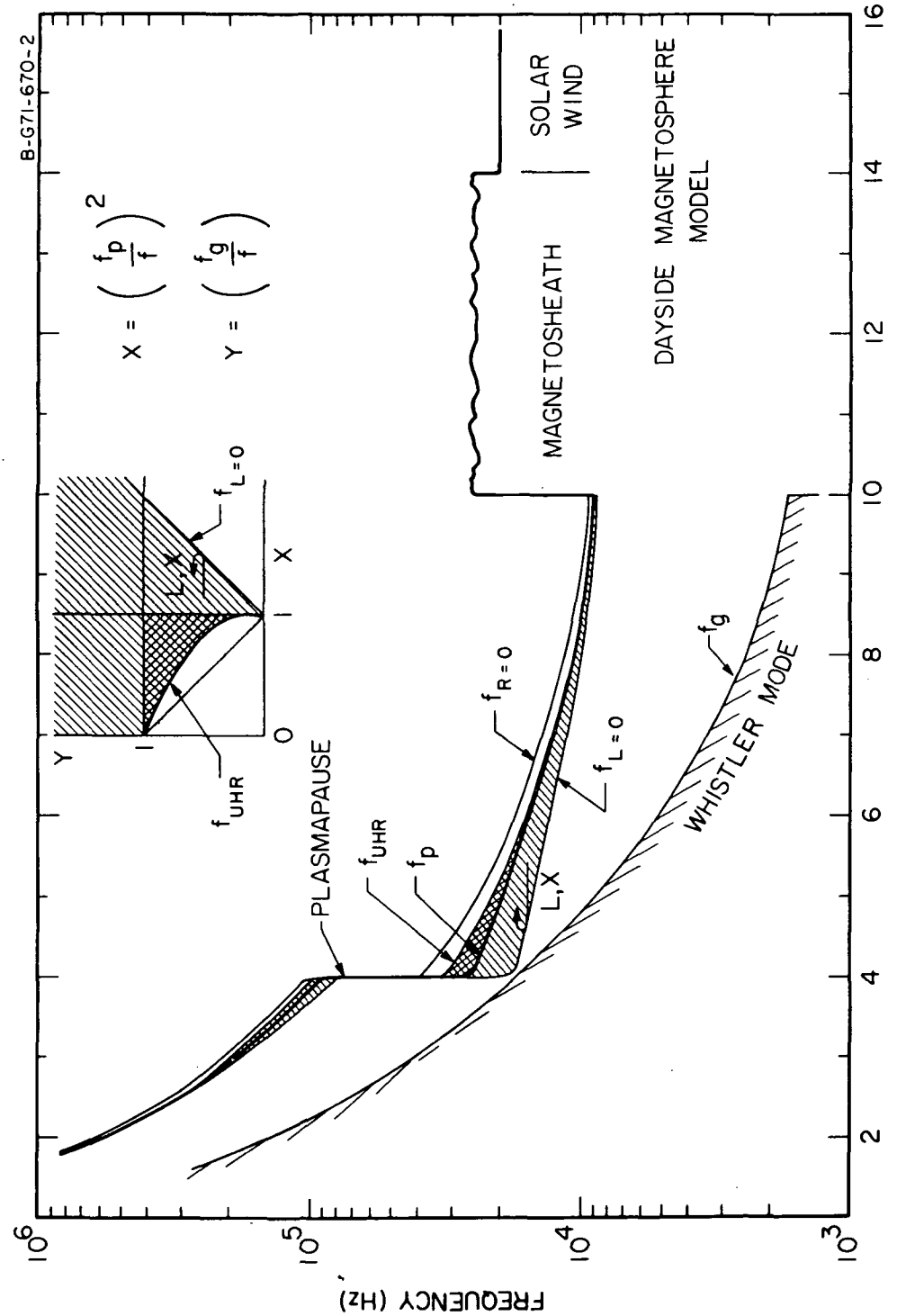
B-G71-670-2
$X = \left(\frac{f_p}{f}\right)^2$
$Y = \left(\frac{f_g}{f}\right)$
$f_{L=0}$
L, X
f_{UHR}
Y
1
0
X
SOLAR WIND
MAGNETOSHEATH
DAYSIDE MAGNETOSPHERE MODEL
PLASMAPAUSE
f_{UHR}
f_p
$f_{R=0}$
$f_{L=0}$
L, X
f_g
WHISTLER MODE
FREQUENCY (Hz)
10^6
10^5
10^4
10^3
2
4
6
8
10
12
14
16
RADIAL DISTANCE (Re)

Figure 5

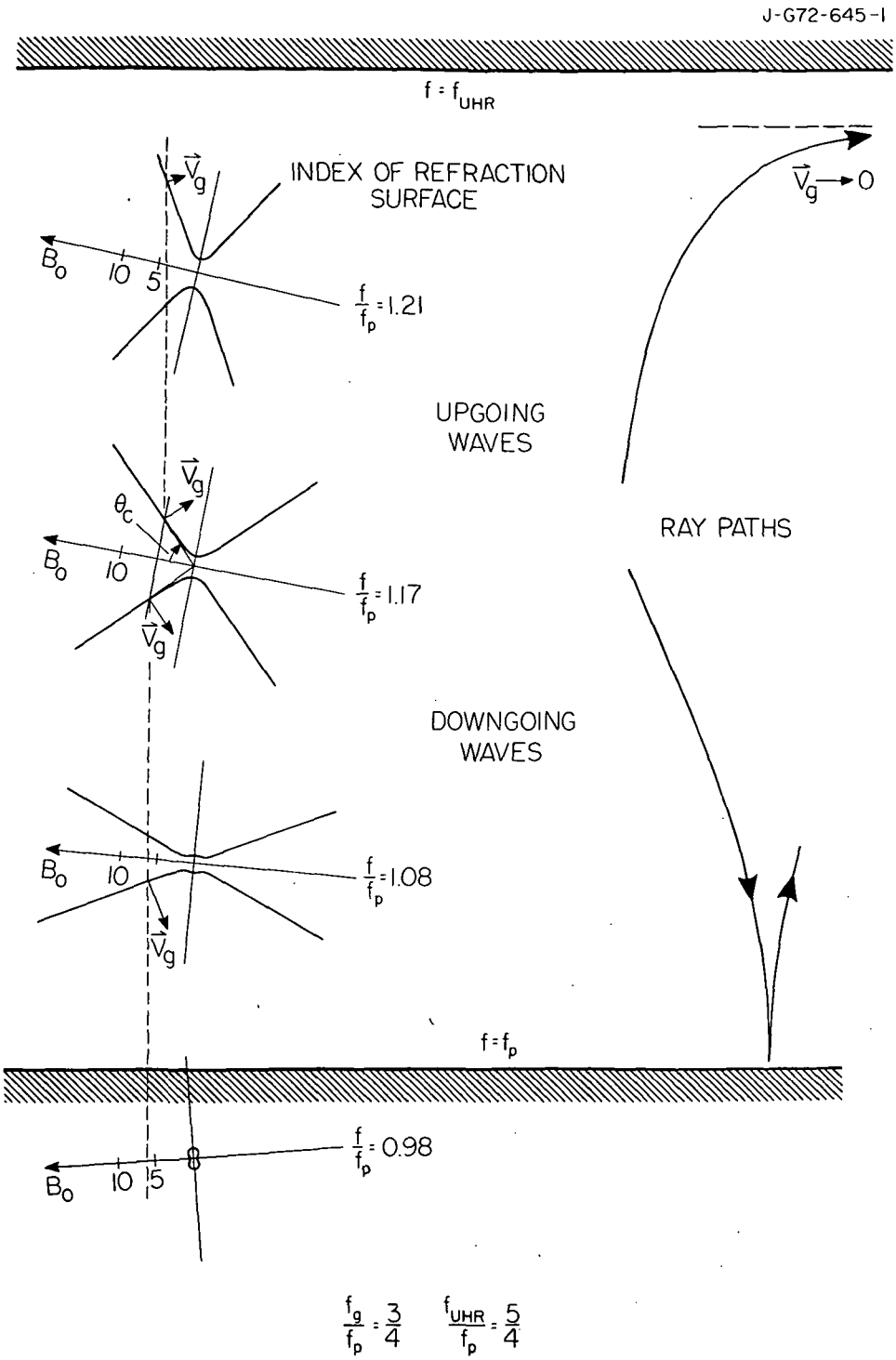
J-G72-645-1
f = f_UHR
INDEX OF REFRACTION SURFACE
V_g
B_0
10
5
f/f_p = 1.21
UPGOING WAVES
θ_c
f/f_p = 1.17
DOWNGOING WAVES
f/f_p = 1.08
f = f_p
f/f_p = 0.98
V_g → 0
RAY PATHS
f_g/f_p = 3/4
f_UHR/f_p = 5/4

Figure 6

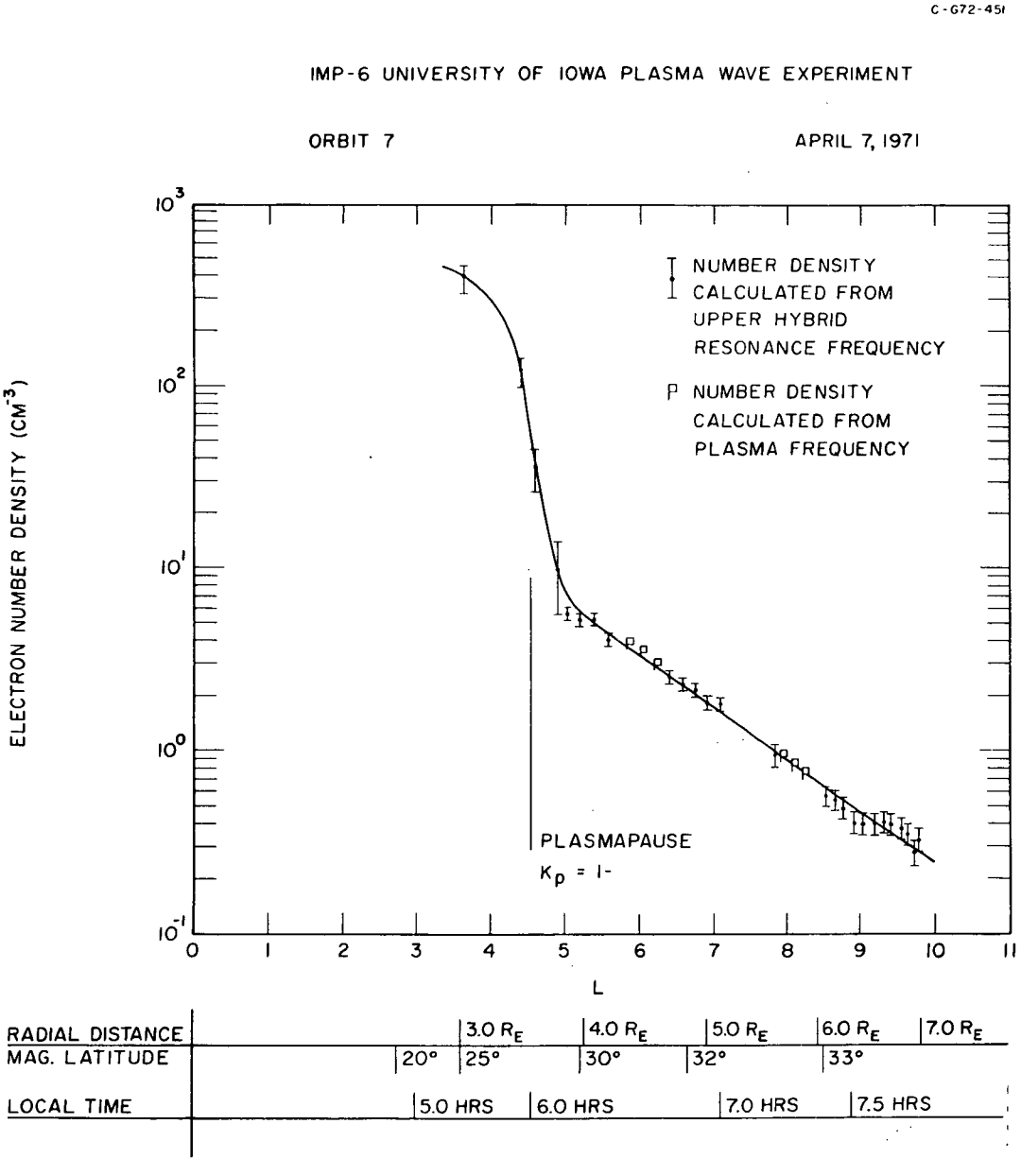
C-G72-451
IMP-6 UNIVERSITY OF IOWA PLASMA WAVE EXPERIMENT
ORBIT 7
APRIL 7, 1971
ELECTRON NUMBER DENSITY (CM⁻³)
10³
10²
10¹
10⁰
10⁻¹
0 1 2 3 4 5 6 7 8 9 10 11
L
NUMBER DENSITY CALCULATED FROM UPPER HYBRID RESONANCE FREQUENCY
P NUMBER DENSITY CALCULATED FROM PLASMA FREQUENCY
PLASMAPAUSE
Kp = 1-
RADIAL DISTANCE
3.0 RE
4.0 RE
5.0 RE
6.0 RE
7.0 RE
MAG. LATITUDE
20°
25°
30°
32°
33°
LOCAL TIME
5.0 HRS
6.0 HRS
7.0 HRS
7.5 HRS

Figure 7

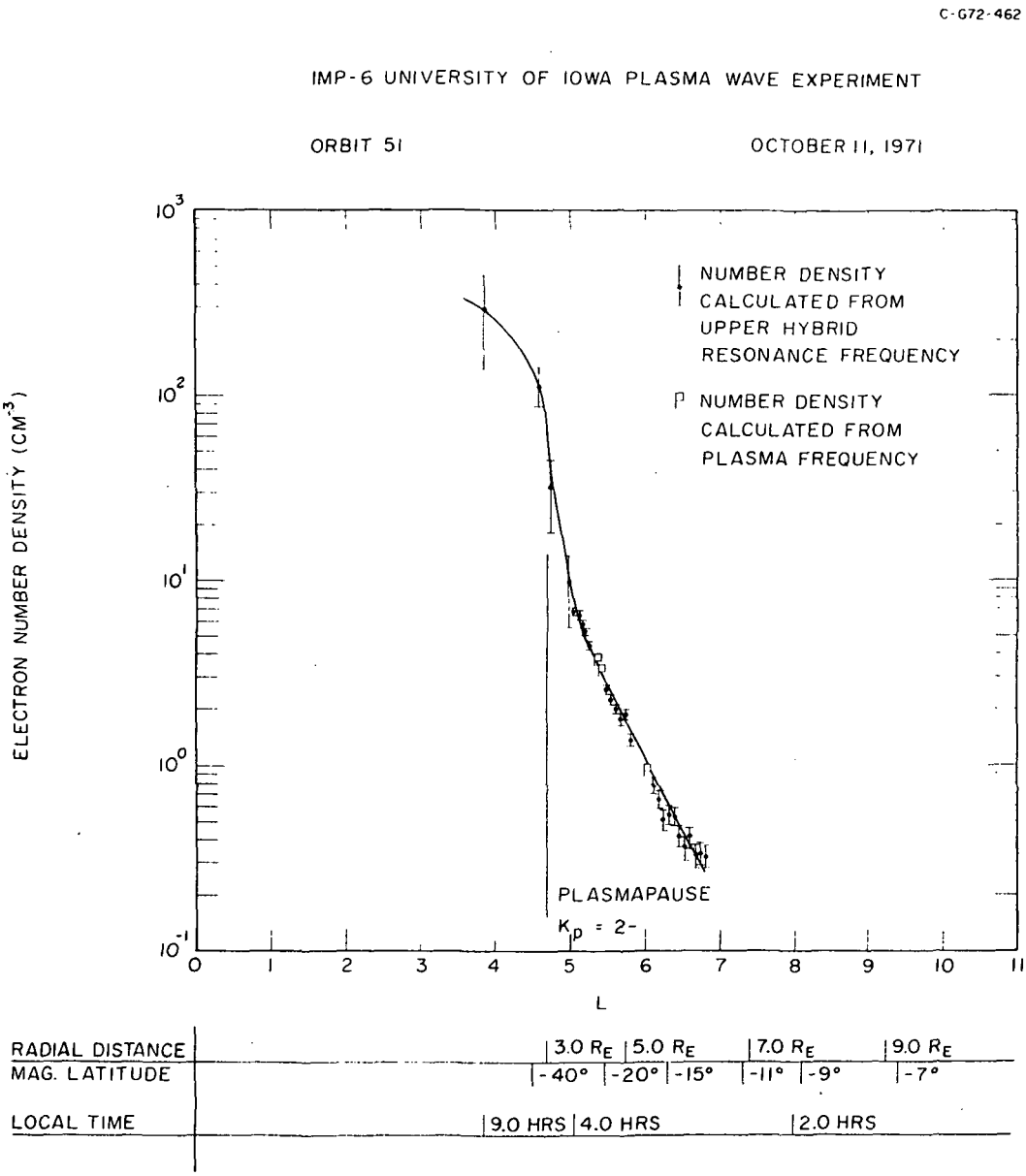
C-G72-462
IMP-6 UNIVERSITY OF IOWA PLASMA WAVE EXPERIMENT
ORBIT 51
OCTOBER 11, 1971
ELECTRON NUMBER DENSITY (CM⁻³)
NUMBER DENSITY CALCULATED FROM UPPER HYBRID RESONANCE FREQUENCY
NUMBER DENSITY CALCULATED FROM PLASMA FREQUENCY
PLASMAPAUSE
Kp = 2-
L
RADIAL DISTANCE
MAG. LATITUDE
LOCAL TIME
3.0 RE
5.0 RE
7.0 RE
9.0 RE
-40°
-20°
-15°
-11°
-9°
-7°
9.0 HRS
4.0 HRS
2.0 HRS

Figure 8